AIMS Mathematics, 9(9): 24109–24142.
DOI: 10.3934/math.20241172
Received: 06 June 2024
Revised: 28 July 2024
Accepted: 31 July 2024
Published: 14 August 2024

http://www.aimspress.com/journal/Math

Research article

Analysis of Weibull progressively first-failure censored data with beta-binomial removals

Refah Alotaibi[1], **Mazen Nassar**[2,*], **Zareen A. Khan**[1] **and Ahmed Elshahhat**[3]

[1] Department of Mathematical Sciences, College of Science, Princess Nourah bint Abdulrahman University, P.O. Box 84428, Riyadh 11671, Saudi Arabia

[2] Department of Statistics, Faculty of Science, King Abdulaziz University, Jeddah 21589, Saudi Arabia

[3] Faculty of Technology and Development, Zagazig University, Zagazig 44519, Egypt

* **Correspondence:** Email: mmohamad3@kau.edu.sa.

Abstract: This study examined the estimations of Weibull distribution using progressively first-failure censored data, under the assumption that removals follow the beta-binomial distribution. Classical and Bayesian approaches for estimating unknown model parameters have been established. The estimations included scale and shape parameters, reliability and failure rate metrics as well as beta-binomial parameters. Estimations were considered from both point and interval viewpoints. The Bayes estimates were developed by using the squared error loss and generating samples for the posterior distribution through the Markov Chain Monte Carlo technique. Two interval estimation approaches are considered: approximate confidence intervals based on asymptotic normality of likelihood estimates and Bayes credible intervals. To investigate the performance of classical and Bayesian estimations, a simulation study was considered by various kinds of experimental settings. Furthermore, two examples related to real datasets were thoroughly investigated to verify the practical importance of the suggested methodologies.

Keywords: Weibull distribution; progressive first-failure censoring; beta-binomial removals; classical estimation; Bayesian estimation
Mathematics Subject Classification: 62F10, 62F15, 62N01, 62N02, 62N05

1. Introduction

In recent years, several censoring approaches have been proposed to overcome the disadvantages of using whole sample data, particularly in reliability/survival analysis for units that fail slowly over time. In cases where the time-to-event is very lengthy and testing resources are limited, but testing

supplies are considerably cheaper, the investigators can employ first-failure censoring (FFC), in which the investigator splits the units into multiple groups, each serving just like a collection of test units, and subsequently runs the test for all groups simultaneously until the first failure in each set is noticed. The sample units can be tested using the formula $n = k \times r$, where r represents the number of groups and k refers to the number of units in each group; see, for more details Balasooriya [1], Wu et al. [2] and Wu et al. [3]. Similar to conventional single censoring schemes, the FFC mechanism prohibits units from being eliminated at any time other than the final cutoff time. However, this assumption is not always valid, as there may be scenarios in which the researcher needs to remove specific units from the test for additional investigation. Wu and Kuş [4] proposed a progressive FFC (PFFC) methodology that combines FFC and progressive Type-II censoring strategies to address that drawback. In other words, the PFFC plan permits the investigator to drop some groups of units from the test before all groups experience their initial failures. Suppose we want to analyze the reliability and failure characteristics of a new batch of semiconductor devices. To efficiently collect reliable data while managing costs and test duration, we can implement the PFFC plan. This plan involves dividing the semiconductor devices into r groups, each containing k units. We then initiate the test and record the occurrence of the first failure. At this point, we stop the test, randomly remove some groups (including the group that experienced the failure), and proceed to the next step. Once the second failure is recorded, we stop the test again, remove additional groups randomly (including the group where the second failure occurred), and repeat this process for subsequent failures. The test concludes after reaching the predetermined number of failures. In the next section, we will delve into this process in more detail. Wu and Kuş [4] checked inferences for the Weibull model and concluded that this censorship yields quicker tests than the conventional progressive Type-II censoring. Many studies considered the PFFC scheme; see, for example Dube et al. [5], Saini et al. [6], Nassar et al. [7], Ashour et al. [8], Eliwa and Ahmed [9], and Alsadat et al. [10].

The PFFC plan assumes that the removal pattern used during the test is fixed. However, in some real-world situations, the removal pattern may happen at random. Yuen and Tse [11] stated that, in some survival/reliability trials, the investigator may determine that it is not suitable or too risky to continue testing on certain tested units, irrespective of whether they have failed. In these situations, the pattern of eliminating after each failure is random. Different approaches have been proposed to address the assumption of a random removal pattern in the case of the PFFC scheme. The first approach utilizes discrete uniform removals, which was demonstrated by Huang and Wu [12]. The second involves binomial removals, as proposed by Ashour et al. [13]. The third approach employs beta-binomial removals (BBR), as suggested by Elshahhat et al. [14]. The first and second approaches might not be appropriate. The first strategy assumes that each removal instance has an equal likelihood, without regard to the number of units discarded. The second strategy assumes that the likelihood of removal for each unit remains constant throughout the test. In the third approach, Elshahhat et al. [14] assumed a binomial distribution for the number of removals and a beta distribution for the likelihood of removals. They termed this approach PFFC with BBR (PFFC-BBR). They considered this scheme to investigate some classical and Bayesian estimation issues for a generalized extreme value lifetime model. It is important to note that the use of BBRs is not commonly employed in various progressive censoring plans. Some available studies are Singh et al. [15], Usta and Gezer [16], Kaushik et al. [17], Vishwakarma et al. [18], and Sangal and Sinha [19]. This may be due to several reasons: (1) the complex formulation of the joint likelihood function, (2) the increased number of unknown parameters,

and (3) the related computational aspects. The detail description of the PFFC-BBR plan is discussed in the next section.

In this study, we assume that the lifespan of the tested units follows a Weibull distribution (WD). The WD is commonly used in reliability studies for modeling time to failure data. It extends the classical exponential distribution to incorporate nonconstant hazard rate shapes. Its hazard rate function (HRF) can be used to model data with increasing or decreasing shapes. It has been effectively employed to explain both early burning failures and failures caused by wearouts. The random variable T is said to have the WD(α, θ) if its probability density function (PDF) is expressed as

$$g(t; \alpha, \theta) = \alpha\theta t^{\alpha-1} e^{-\theta t^{\alpha}}, t > 0, \alpha, \theta > 0, \tag{1.1}$$

where α and θ are shape and scale parameters, respectively. The cumulative distribution function (CDF) related to (1.1) is given by

$$G(t; \alpha, \theta) = 1 - e^{-\theta t^{\alpha}}. \tag{1.2}$$

In addition, the reliability function (RF) and HRF of the random variable T, are given, respectively by

$$R(t; \alpha, \theta) = e^{-\theta t^{\alpha}} \text{ and } h(t; \alpha, \theta) = \alpha\theta t^{\alpha-1}. \tag{1.3}$$

The WD can take on various forms depending on the value of its shape parameter, α. When $\alpha = 1$, the WD reduces to the exponential distribution. When $\alpha = 2$, the WD matches the Rayleigh distribution. Due to its wide range of applications, researchers use it in various contexts, such as quality control, reliability analysis, medical investigations, and engineering studies. Given the WD's popularity and usefulness, several publications investigated its classical and Bayesian estimation issues using various types of data. Some recent studies include Jia et al. [20], Nassar et al. [21], Ramos et al. [22], Zhu [23], Starling et al. [24], Ren and Gui [25], and Nassar and Elshahhat [26].

It is worth noting that only a few studies have considered the PFFC-BBR plan, despite its significance in life-testing experiments. Furthermore, despite the prevalence of WD as one of the most popular lifetime models, no study has examined its estimation issues in the context of the PFFC-BBR plan. Taking these reasons into consideration, we are inspired to conduct this study because of the importance and wide applications of the WD as a lifetime model, as well as the importance of the PFFC-BBR plan which is more practical than the PFFC plan with prefixed removal. The key objective of this research is to draw inferences about the parameters of the WD under the PFFC-BBR plan. From this objective, we can list our sub-objectives, as shown below:

1) Considering the maximum likelihood estimation approach to get the maximum likelihood estimates (MLEs) of the unknown parameters, including the RF. The approximate confidence intervals (ACIs) are also addressed. The ACI of the RF is produced via employing the delta method (DM) to approximate the variance of its MLE.
2) Investigating Bayesian estimations for various parameters. This involves obtaining both Bayes estimates (BEs) and Bayes credible intervals (BCIs). The BEs are calculated based on the squared error (SE) loss function. The Markov Chain Monte Carlo (MCMC) technique is recommended for extracting samples from conditional distributions in order to produce the necessary BEs and BCIs.
3) Comparing the point estimates, namely, MLEs and BEs, and interval ranges, including ACIs and BCIs, of the unknown parameters by Monte Carlo simulations. The simulation considered various parameter values, sample sizes, and removal patterns.

4) Applying the provided estimates to actual datasets. This analysis aids in demonstrating the applicability of the offered approaches in real-world settings.

The remaining parts of this study are arranged as follows: Section 2 depicts the framework of the PFFC-BBR scheme. Section 3 discusses the WD's MLEs and ACIs based on the PFFC-BBR plan. Section 4 discusses the various Bayesian estimates. Section 5 describes the simulations' design and findings. Section 6 investigates two real-world datasets. Finally, in Section 7, we provide a conclusion to the study.

2. Designing the PFFC-BBR plan

This section describes the design of the PFFC-BBR plan. Before progressing further, this example demonstrates why the beta-binomial distribution is used to model the removal pattern instead of the beta distribution. Consider a clinical study where the likelihood of participants dropping out can vary depending on when deaths are reported. If deaths occur early in the study, there will initially be a high chance of removals, which may decrease over time. On the other hand, if all patients survive for a longer period and the first death occurs much later, the probability of dropout will be relatively small at the beginning and may increase later on. This fluctuation in dropout probability at each stage of the experiment indicates that it is not constant throughout the entire study. Therefore, it is necessary to consider the number of removals as a random variable, following a binomial distribution at each stage with a randomly distributed probability of removal. To account for the uncertainty in the probability of removal at different stages of the experiment, we have used beta distribution, which can take on a wide range of shapes, to model this variability. By combining the distribution of the number of removals with the probability of removal, we obtain a beta-binomial distribution for S_i. Assume that r distinct groups, each with k units, are placed through a life-testing experiment at age zero. Suppose that d is a predetermined number of failures and $\mathbf{S} = (S_1, \ldots, S_d)$ represent the groups' random removal pattern. When the time of the first failure, say $T_{1:d}$, occurs, some S_1 groups are excluded from the experiment, including the group that experienced the first failure. Following the time of the second failure $T_{2:d}$, some S_2 groups, including the group with the second failure, are deleted from the surviving live $r - S_1 - 1$ groups, and so on. The process runs until the d^{th} failure takes place and at the failure time $T_{d:d}$, all the surviving groups, given by $S_d = r - d - \sum_{i=1}^{d-1} S_i$, are removed from the test.

Let $\mathbf{T} = (T_{1:d}, \ldots, T_{d:d})$ denote the independent lifetimes of the PFFC order statistics with a pre-fixed removal pattern $(S_1 = s_1, \ldots, S_d = s_d)$ obtained from the Weibull population. Then, the joint likelihood function (LF) of the observed data can be written, ignoring the constant term, as follows:

$$L_1(\alpha, \theta; \mathbf{t}|\mathbf{S}) = \prod_{i=1}^{d} g(t_i; \alpha, \theta) \left[1 - G(t_i; \alpha, \theta)\right]^{k(s_i+1)-1}, \tag{2.1}$$

where $\mathbf{t}$ is the realization of $\mathbf{T}$ and $t_i = t_{i:d}, i = 1, \ldots, d$, for the sake of simplicity. At the i^{th} failure, with $i = 1, \ldots, d-1$, assume that the likelihood of the removal s_i follows the binomial distribution with parameters $r - d - \sum_{j=1}^{i-1} s_j$ and π with the following probability mass function (PMF):

$$\Pr(\mathbf{S} = \mathbf{s}|\pi) = \binom{n_i^*}{s_i} \pi^{s_i} (1-\pi)^{n_i^\star}, i = 1, 2, \ldots, d-1, \tag{2.2}$$

where $n_i^* = r - d - \sum_{j=1}^{i-1} s_j$, $n_i^\star = r - d - \sum_{j=1}^{i} s_j$, $0 \leqslant s_1 \leqslant r - d$ and $0 \leqslant s_i \leqslant n_i^*$ for $i = 2, 3, \ldots, d-1$. Moreover, it is assumed that the likelihood of removals π follows beta distribution with parameters a and b with PDF expressed as follows:

$$f(\pi|a,b) = \frac{1}{B(a,b)}\pi^{a-1}(1-\pi)^{b-1},\ a,b>0,\ 0<\pi<1, \tag{2.3}$$

where $B(a,b)$ is the beta function. Utilizing (2.2) and (2.3), the unconditional distribution of $S_i's$ is given by

$$\Pr(\mathbf{S}=\mathbf{s}|\,a,b) = \frac{1}{B(a,b)}\binom{n_i^*}{s_i}\int_0^1 \pi^{a+s_i-1}(1-\pi)^{b+n_i^\star-1}\,d\pi.$$

Following some simplifications, we acquire

$$\Pr(\mathbf{S}=\mathbf{s}|\,a,b) = \binom{n_i^*}{s_i}\frac{B\left(a+r_i, b+n_i^\star\right)}{B(a,b)}. \tag{2.4}$$

The PMF in (2.4) corresponds to the beta-binomial distribution, given by $\mathrm{BB}(n_i^*, a, b)$, where n^* is the number of trials. Consequently, the joint probability distribution of BBRs can be determined as

$$\begin{aligned} L_2(\mathbf{S}=\mathbf{s}|\,a,b) = &\Pr(S_1=s_1)\times\Pr(S_2=s_2|\,S_1=s_1)\\ &\times\cdots\times\Pr(S_{d-1}=s_{d-1}|\,S_{d-2}=r_{d-2},\ldots,S_1=d_1). \end{aligned} \tag{2.5}$$

Substituting (2.4) in (2.5), the joint probability of $S_1 = s_1, \ldots, S_d = s_d$ can be written, ignoring the constant term, as

$$L_2(\mathbf{S}=\mathbf{s}|\,a,b) = \frac{1}{[B(a,b)]^{d-1}}\prod_{i=1}^{d-1} B\left(a+s_i, b+n_i^\star\right). \tag{2.6}$$

We also assume that $S_i's$ are independent of $T_i's$ for all i. In this case, one can write the full LF based on (2.1) and (2.6) as follows:

$$L(\alpha,\theta,a,b;\mathbf{t}|\,\mathbf{S}) = L_1(\alpha,\theta;\mathbf{t}|\,\mathbf{S})\,L_2(\mathbf{S}=\mathbf{s}|\,a,b). \tag{2.7}$$

It is evident that $L_1(\alpha,\theta;\mathbf{t}|\,\mathbf{S})$ is a function of the unknown parameter α and θ of the used lifetime model exclusively, while $L_2(\mathbf{S}=\mathbf{s}|\,a,b)$ is a function of the parameters a and b only. Thus, these functions can be maximized separately to get the MLEs of α, θ, a and b, denoted by $\hat{\alpha}, \hat{\theta}, \hat{a}$ and $\hat{b}$, respectively.

3. Classical inference

This part focuses on estimations of α, θ, a and b as well as RF and HRF of the WD using PFFC-BBR data. All of these quantities will now be handled as unknown parameters. Both MLEs and ACIs for the unknown parameters are examined in this part.

3.1. Point estimation

Employ a PFFC-BBR sample $\mathbf{t}$ of size d selected from a Weibull population with PDF and CDF given by (1.1) and (1.2), respectively. Then, the LF of α and θ can be expressed using (2.1) as follows

$$L_1(\alpha, \theta; \mathbf{t}|\mathbf{S}) = \alpha^d \theta^d \exp\left[(\alpha - 1)\sum_{i=1}^{d} \log(t_i) - \theta \sum_{i=1}^{d} m_i t_i^{\alpha}\right], \tag{3.1}$$

where $m_i = k(s_i + 1)$. The natural logarithm of LF in (3.1) is

$$\mathfrak{L}_1(\alpha, \theta; \mathbf{t}|\mathbf{S}) = d\log(\alpha) + d\log(\theta) + (\alpha - 1)\sum_{i=1}^{d} \log(t_i) - \theta \sum_{i=1}^{d} m_i t_i^{\alpha}. \tag{3.2}$$

On the other hand, employing the relation $B(v, u) = \Gamma(v)\Gamma(u)/\Gamma(v + u)$, where $\Gamma(.)$ refers to the gamma function, the natural logarithm of $L_2(\mathbf{S} = \mathbf{s}|\, a, b)$ in (2.6) can be expressed as follows:

$$\begin{aligned}\mathfrak{L}_2(\mathbf{S} = \mathbf{s}|\, a, b) \;=\; & (d-1)\log[\Gamma(a+b)] - (d-1)\left[\log[\Gamma(a)] + \log[\Gamma(b)]\right] + \sum_{i=1}^{d-1} \log[\Gamma(a + s_i)] \\ & + \sum_{i=1}^{d-1} \log[\Gamma(b + n^{\star})] - \sum_{i=1}^{d-1} \log[\Gamma(a + s_i + b + n^{\star})].\end{aligned} \tag{3.3}$$

Now, the MLEs of α and θ can be obtained by simultaneously solving the following normal equations:

$$\frac{\partial \mathfrak{L}_1(\alpha, \theta; \mathbf{t}|\mathbf{S})}{\partial \alpha} = \frac{d}{\alpha} + \sum_{i=1}^{d} \log(t_i) - \theta \sum_{i=1}^{d} m_i t_i^{\alpha} \log(t_i) = 0 \tag{3.4}$$

and

$$\frac{\partial \mathfrak{L}_1(\alpha, \theta; \mathbf{t}|\mathbf{S})}{\partial \alpha} = \frac{d}{\theta} - \sum_{i=1}^{d} m_i t_i^{\alpha} = 0. \tag{3.5}$$

From (3.5), the MLE $\hat{\theta}$ can be acquired as a function of the MLE $\hat{\alpha}$ as follows:

$$\hat{\theta} = \frac{d}{\sum_{i=1}^{d} m_i t_i^{\hat{\alpha}}}. \tag{3.6}$$

Equation (3.4), when combined with the MLE of $\hat{\theta}$ in (3.6), reduces to

$$\frac{1}{\hat{\alpha}} + \frac{1}{d}\sum_{i=1}^{d} \log(t_i) - \frac{\sum_{i=1}^{d} m_i t_i^{\hat{\alpha}} \log(t_i)}{\sum_{i=1}^{d} m_i t_i^{\hat{\alpha}}} = 0. \tag{3.7}$$

It is observed that Eq (3.7) cannot be solved analytically for $\hat{\alpha}$. Its numerical solution can be accomplished by employing the following iterative process

$$\hat{\alpha}^{(j+1)} = \left[\frac{\sum_{i=1}^{d} m_i t_i^{\hat{\alpha}^{(j)}} \log(t_i)}{\sum_{i=1}^{d} m_i t_i^{\hat{\alpha}^{(j)}}} - \frac{1}{d}\sum_{i=1}^{d} \log(t_i)\right]^{-1},$$

where $\hat{\alpha}^{(j)}$ is the MLE of α at iteration number j. Once getting the MLE $\hat{\alpha}$, the MLE $\hat{\theta}$ can be simply obtained from (3.6).

In Figure 1, by plotting the profile log-likelihood curves of α and θ, the existence and uniqueness of their acquired MLEs $\hat{\alpha}$ and $\hat{\theta}$ are proved. The subplots shown in Figure 1 are created using a simulated PFFC-BBR sample generated from WD(0.25,0.75) and BB(2, 5) when $(r, d, k) = (40, 10, 2)$. It indicates that the estimates $\hat{\alpha} \simeq 0.3213$ and $\hat{\theta} \simeq 0.4952$ exist and are unique.

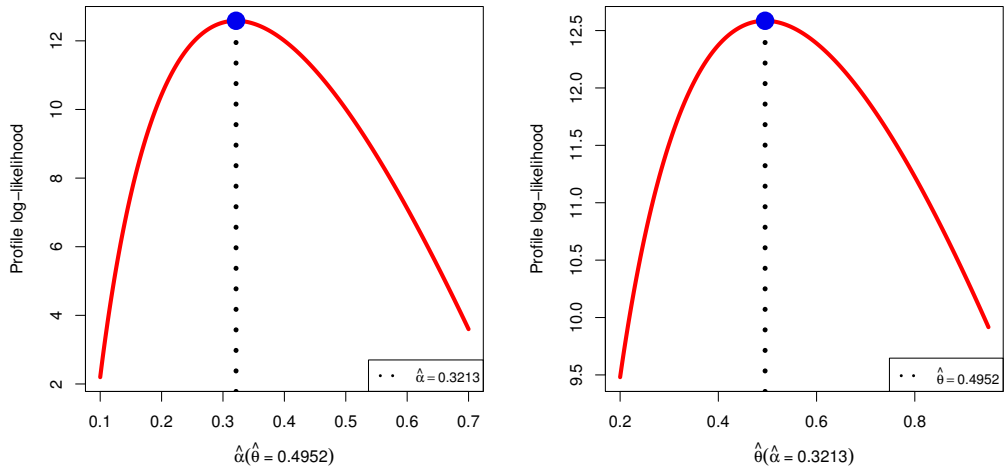

Figure 1. The log-likelihood curves of α (left) and θ (right) from the simulated data.

In contrast, the MLEs $\hat{a}$ and $\hat{b}$ can be derived as the simultaneous solution of the two subsequent normal nonlinear equations

$$\frac{\partial \mathfrak{L}_2\left(\mathbf{S}=\mathbf{s}|\, a, b\right)}{\partial a} = (d-1)[\psi(a+b)-\psi(a)] + \sum_{i=1}^{d-1}\psi(a+s_i) - \sum_{i=1}^{d-1}\psi(a+s_i+b+n_i^{\star}) = 0 \qquad (3.8)$$

and

$$\frac{\partial \mathfrak{L}_2\left(\mathbf{S}=\mathbf{s}|\, a, b\right)}{\partial b} = (d-1)[\psi(a+b)-\psi(b)] + \sum_{i=1}^{d-1}\psi(b+n_i^{\star}) - \sum_{i=1}^{d-1}\psi(a+s_i+b+n_i^{\star}) = 0, \qquad (3.9)$$

where $\psi[\xi(x)] = \partial \log \Gamma(\xi(x))/\partial x$ is the digamma function.

It is clear that the MLEs $\hat{a}$ and $\hat{b}$ cannot be acquired directly from (3.8) and (3.9). As a result, the required estimates can be obtained using any suitable numerical technique. By leveraging the MLEs $\hat{\alpha}$ and $\hat{\theta}$ with the invariance trait of the MLEs, the MLEs of RF and HRF of the WD, at time t_0, can be computed from (1.3) as follows:

$$\hat{R}(t_0) = e^{-\hat{\theta}t_0^{\hat{\alpha}}} \quad \text{and} \quad h(t_0) = \hat{\alpha}\hat{\theta}t_0^{\hat{\alpha}-1}.$$

3.2. Interval estimation

Here, we employ the asymptotic normality of the MLEs to construct the ACIs of the various unknown parameters. To obtain such intervals, we first need the following elements obtained from $\mathfrak{L}_1(\alpha, \theta|\mathbf{S}, \mathbf{t})$ and $\mathfrak{L}_2(\mathbf{S} = \mathbf{s}|\, a, b)$,

$$\frac{\partial^2 \mathfrak{L}_1(\alpha, \theta; \mathbf{t}|\mathbf{S})}{\partial \alpha^2} = -\frac{d}{\alpha^2} - \theta \sum_{i=1}^{d} m_i t_i^{\alpha} \log^2(t_i),$$

$$\frac{\partial^2 \mathfrak{L}_1(\alpha, \theta; \mathbf{t}|\mathbf{S})}{\partial \alpha^2} = -\frac{d}{\theta^2}, \quad \frac{\partial^2 \mathfrak{L}_1(\alpha, \theta; \mathbf{t}|\mathbf{S})}{\partial \alpha \partial \theta} = -\sum_{i=1}^{d} m_i t_i^{\alpha} \log(t_i),$$

$$\frac{\partial^2 \mathfrak{L}_2(\mathbf{S} = \mathbf{s}|\, a, b)}{\partial a^2} = (d-1)[\psi_1(a+b) - \psi_1(a)] + \sum_{i=1}^{d-1} \psi_1(a + s_i) - \sum_{i=1}^{d-1} \psi_1(a + s_i + b + n_i^{\star}),$$

$$\frac{\partial^2 \mathfrak{L}_2(\mathbf{S} = \mathbf{s}|\, a, b)}{\partial b^2} = (d-1)[\psi_1(a+b) - \psi_1(b)] + \sum_{i=1}^{d-1} \psi_1(b + n_i^{\star}) - \sum_{i=1}^{d-1} \psi_1(a + s_i + b + n_i^{\star})$$

and

$$\frac{\partial^2 \mathfrak{L}_2(\mathbf{S} = \mathbf{s}|\, a, b)}{\partial a \partial b} = (d-1)\psi_1(a+b) - \sum_{i=1}^{d-1} \psi_1(a + s_i + b + n_i^{\star}),$$

where $\psi_1[\xi(x)] = \partial^2 \log \Gamma(\xi(x))/\partial x^2$ is the trigamma function. Under some mild conditions, the distribution of the MLEs $(\hat{\alpha}, \hat{\theta}, \hat{a}, \hat{b})$ are multivariate normal with mean equals to the true parameter values and covariance matrix $\mathbf{I}^{-1}(\alpha, \theta, a, b)$. In practice, we commonly estimate $\mathbf{I}^{-1}(\alpha, \theta, a, b)$ by $\mathbf{I}^{-1}(\hat{\alpha}, \hat{\theta}, \hat{a}, \hat{b})$ in order to avoid deriving the exact expressions of the Fisher information matrix, which are quite challenging in this situation. Thus, $\mathbf{I}^{-1}(\hat{\alpha}, \hat{\theta}, \hat{a}, \hat{b})$ can be expressed as follows:

$$\mathbf{I}^{-1}(\hat{\alpha}, \hat{\theta}, \hat{a}, \hat{b}) = \begin{bmatrix} \widehat{var}(\hat{\alpha}) & \widehat{cov}(\hat{\alpha}, \hat{\theta}) & 0 & 0 \\ \widehat{cov}(\hat{\theta}, \hat{\alpha}) & \widehat{var}(\hat{\theta}) & 0 & 0 \\ 0 & 0 & \widehat{var}(\hat{a}) & \widehat{cov}(\hat{a}, \hat{b}) \\ 0 & 0 & \widehat{cov}(\hat{b}, \hat{a}) & \widehat{var}(\hat{b}) \end{bmatrix}. \tag{3.10}$$

The estimated covariance matrix in (3.10) is computed by taking the inverse of the observed Fisher information matrix, whose elements are evaluated at the MLEs $\hat{\alpha}, \hat{\theta}, \hat{a}$, and $\hat{b}$. Then, with $100(1-\tau)\%$ confidence level, the ACIs for the parameters α, θ, a, and b are

$$\left[\hat{\alpha} - z_{\tau/2}\sqrt{\widehat{var}(\hat{\alpha})},\ \hat{\alpha} + z_{\tau/2}\sqrt{\widehat{var}(\hat{\alpha})}\right],\ \left[\hat{\theta} - z_{\tau/2}\sqrt{\widehat{var}(\hat{\theta})},\ \hat{\theta} + z_{\tau/2}\sqrt{\widehat{var}(\hat{\theta})}\right]$$

and

$$\left[\hat{a} - z_{\tau/2}\sqrt{\widehat{var}(\hat{a})},\ \hat{a} + z_{\tau/2}\sqrt{\widehat{var}(\hat{a})}\right],\ \left[\hat{b} - z_{\tau/2}\sqrt{\widehat{var}(\hat{b})},\ \hat{b} + z_{\tau/2}\sqrt{\widehat{var}(\hat{b})}\right],$$

where $z_{\tau/2}$ is the upper $\tau/2$ percentile of the standard normal distribution. Regarding the ACIs of the reliability metrics, we need to get estimates of the variances associated with their MLEs $\hat{R}(t_0)$ and $\hat{h}(t_0)$. Here, we use the DM to approximate the estimated variances. Let $\widehat{var}(\hat{R})$ and $\widehat{var}(\hat{h})$ represent

the required estimated variances of $\hat{R}(t_0)$ and $\hat{h}(t_0)$, respectively. Using the DM, we can approximate them as follows:

$$\begin{aligned}\widehat{var}(\hat{R}) &\approx \begin{pmatrix} \hat{R}_1 & \hat{R}_2 \end{pmatrix}\begin{pmatrix} \widehat{var}(\hat{\alpha}) & \widehat{cov}(\hat{\alpha},\hat{\theta}) \\ \widehat{cov}(\hat{\theta},\hat{\alpha}) & \widehat{var}(\hat{\theta}) \end{pmatrix}\begin{pmatrix} \hat{R}_1 \\ \hat{R}_2 \end{pmatrix} \\ &\approx \hat{R}_1^2\widehat{var}(\hat{\alpha}) + 2\hat{R}_1\hat{R}_2\widehat{cov}(\hat{\alpha},\hat{\theta}) + \hat{R}_2^2\widehat{var}(\hat{\theta})\end{aligned}$$

and

$$\begin{aligned}\widehat{var}(\hat{h}) &\approx \begin{pmatrix} \hat{h}_1 & \hat{h}_2 \end{pmatrix}\begin{pmatrix} \widehat{var}(\hat{\alpha}) & \widehat{cov}(\hat{\alpha},\hat{\theta}) \\ \widehat{cov}(\hat{\theta},\hat{\alpha}) & \widehat{var}(\hat{\theta}) \end{pmatrix}\begin{pmatrix} \hat{h}_1 \\ \hat{h}_2 \end{pmatrix} \\ &\approx \hat{h}_1^2\widehat{var}(\hat{\alpha}) + 2\hat{h}_1\hat{h}_2\widehat{cov}(\hat{\alpha},\hat{\theta}) + \hat{h}_2^2\widehat{var}(\hat{\theta}),\end{aligned}$$

where

$$\hat{R}_1 = -\hat{\theta}t_0^{\hat{\alpha}}e^{-\hat{\theta}t_0^{\hat{\alpha}}}\log(t_0),\ \ \hat{R}_2 = -t_0^{\hat{\alpha}}e^{-\hat{\theta}t_0^{\hat{\alpha}}}$$

and

$$\hat{h}_1 = \hat{\theta}t_0^{\hat{\alpha}-1}[1+\hat{\alpha}\log(t_0)],\ \ \hat{h}_2 = \hat{\alpha}t_0^{\hat{\alpha}-1}.$$

Then, the $100(1-\tau)\%$ ACIs for the parameters RF and HRF are

$$\left[\hat{R} - z_{\tau/2}\sqrt{\widehat{var}(\hat{R})},\ \hat{R} + z_{\tau/2}\sqrt{\widehat{var}(\hat{R})}\right] \text{ and } \left[\hat{h} - z_{\tau/2}\sqrt{\widehat{var}(\hat{h})},\ \hat{h} + z_{\tau/2}\sqrt{\widehat{var}(\hat{h})}\right].$$

4. Bayesian inference

This section explores Bayesian estimation for the different parameters of the WD using PFFC-BBR data. The BEs and BCIs are obtained using the MCMC technique, as their closed expressions cannot be explicitly derived from the posterior distribution. It is important in Bayesian analysis to choose the appropriate prior distribution that reflects our knowledge about the unknown parameters. Let's begin by considering the unknown parameters α and θ. We assume that these two variables are independent and each follows a gamma distribution. The joint prior distribution in this case is as follows:

$$\phi_1(\alpha,\theta) \propto \alpha^{\nu_1-1}\theta^{\nu_2-1}e^{-(\omega_1\alpha+\omega_2\theta)}, \alpha,\theta > 0, \tag{4.1}$$

where the hyperparameters $\nu_j, \omega_j > 0, j = 1,2$ are assumed to be known. For more detail about the importance of Bayesian reliability estimation, see Xu et al. [27]. From (3.1) and (4.1), one can formulate the joint posterior distribution of α and θ as follows:

$$Q_1(\alpha,\theta|\mathbf{S},\mathbf{t}) = \frac{1}{A_1}\alpha^{d+\nu_1-1}\theta^{d+\nu_2-1}\exp\left[\alpha\left[\sum_{i=1}^{d}\log(t_i) - \omega_1\right] - \theta\left(\sum_{i=1}^{d} m_i t_i^{\alpha} + \omega_2\right)\right], \tag{4.2}$$

where A_1 refers to the normalized constant. On the other hand, for the unknown parameters a and b, it is assumed that they are independent and follow the gamma prior distribution, with the following joint prior distribution

$$\phi_2(a,b) \propto a^{\nu_3-1}b^{\nu_4-1}e^{-(\omega_3 a+\omega_4 b)}, a,b > 0, \tag{4.3}$$

where $\nu_j, \omega_j, j = 3, 4$ are known and positive. The joint posterior distribution of a and b can be expressed using Eqs (2.6) and (4.3)

$$Q_2(a, b|\mathbf{S} = \mathbf{s}) = \frac{a^{\nu_3-1} b^{\nu_4-1} e^{-(\omega_3 a+\omega_4 b)}}{A_2[B(a, b)]^{d-1}} \prod_{i=1}^{d-1} B\left(a + s_i, b + n^{\star}\right), \tag{4.4}$$

where A_2 is the normalized constant. It is clear that the BEs and BCIs of the parameters α, θ RF and HRF can be acquired from the joint posterior distribution in (4.2). For simplicity, let $\varpi_1(\alpha, \theta)$ be any function of the parameters α and θ.

Then, based on the SE loss function, the BE of $\varpi_1(a, b)$, denoted by $\tilde{\varpi}_1(\alpha, \theta)$, can be computed as

$$\tilde{\varpi}_1(\alpha, \theta) = \int_0^{\infty} \int_0^{\infty} \varpi_1(\alpha, \theta) Q_1(\alpha, \theta|\mathbf{S}, \mathbf{t}) d\alpha \, d\theta. \tag{4.5}$$

Similarly, from the joint posterior in (4.4), the BE of any function of a and b, say $\varpi_2(a, b)$, can be computed based on the SE loss function as

$$\tilde{\varpi}_2(a, b) = \int_0^{\infty} \int_0^{\infty} \varpi_2(a, b) Q_2(a, b|\mathbf{S} = \mathbf{s}) da \, db. \tag{4.6}$$

Since choosing a symmetric (or asymmetric) loss is one of the most important challenges of Bayesian analysis, we recommend considering other loss functions instead of the SE loss, which can be easily incorporated.

It is evident that obtaining the BEs in (4.5) and (4.6) is not straightforward due to the involvement of complex integrals. In such cases, one approach to obtain BEs is through the use of Monte Carlo integration. However, it should be noted that this technique requires more computational time, especially when dealing with a high number of parameters like in our case. Another approach to address this challenge is by implementing the MCMC technique. This method enables the generation of a large sequence of samples which can be used to compute the desired BEs and BCIs. To apply the MCMC technique, we must first derive the full conditional distributions of the different parameters. The full conditional distribution for each parameter is obtained by excluding any quantities that do not rely on the parameter being considered. From the joint posterior distribution in (4.2), the full conditional distributions of α and θ can be expressed, respectively, as

$$Q_1(\alpha|\theta, \mathbf{S}, \mathbf{t}) \propto \alpha^{d+\nu_1-1} \exp\left[\alpha\left[\sum_{i=1}^{d} \log(t_i) - \omega_1\right] - \theta \sum_{i=1}^{d} m_i t_i^{\alpha}\right] \tag{4.7}$$

and

$$Q_1(\theta|\alpha, \mathbf{S}, \mathbf{t}) \propto \theta^{d+\nu_2-1} \exp\left[-\theta\left(\sum_{i=1}^{d} m_i t_i^{\alpha} + \omega_2\right)\right]. \tag{4.8}$$

Similarly, using the joint posterior distribution in (4.4), we can express the full conditional distributions of a and b, respectively, as

$$Q_2(a|b, \mathbf{S} = \mathbf{s}) \propto \frac{a^{\nu_3-1}}{[B(a, b)]^{d-1}} \exp\left[\sum_{i=1}^{d-1} \log[B(a + s_i, b + n_i^{\star})] - \omega_3 a\right] \tag{4.9}$$

and

$$Q_2(b|a, \mathbf{S} = \mathbf{s}) \propto \frac{b^{\nu_4 - 1}}{[B(a,b)]^{d-1}} \exp\left[\sum_{i=1}^{d-1} \log[B(a + s_i, b + n_i^{\star})] - \omega_4 b\right]. \tag{4.10}$$

The following observations are made during the initial check of the full conditional distributions in (4.7)–(4.10):

- From (4.8), it is clear that $\theta \sim Gamma[d + \nu_2, \varrho(\alpha)]$, where $\varrho(\alpha) = \sum_{i=1}^{d} m_i t_i^{\alpha} + \omega_2$. Therefore, to obtain samples of θ, it is possible to use Gibbs sampling.
- The conditional distributions of α, a and b in (4.7), (4.9), and (4.10), respectively, cannot be simplified to any standard distribution. Therefore, we suggest using the Metropolis-Hastings (MH) algorithm to generate the necessary samples from $Q_1(\alpha|\theta, \mathbf{S}, \mathbf{t})$, $Q_2(a|b, \mathbf{S} = \mathbf{s})$, and $Q_2(b|a, \mathbf{S} = \mathbf{s})$.

To apply the MH steps, we consider the normal distribution as a proposal distribution for the three parameters α, a, and b. The MH within Gibbs sampling requires the following processes to generate the MCMC samples

Step 1. Put $j = 1$ and the initial values $(\alpha^{(0)}, \theta^{(0)}, a^{(0)}, b^{(0)}) = (\hat{\alpha}, \hat{\theta}, \hat{a}, \hat{b})$.

Step 2. Implement the MH algorithm to simulate:

- $\alpha^{(j)}$ from $Q_1(\alpha|\theta, \mathbf{S}, \mathbf{t})$ in (4.7);
- $a^{(j)}$ from $Q_2(a|a, \mathbf{S} = \mathbf{s})$ in (4.9);
- $b^{(j)}$ from $Q_2(b|a, \mathbf{S} = \mathbf{s})$ in (4.10).

Step 3. Generate $\theta^{(j)}$ using $Gamma[d + \nu_2, \varrho(\alpha^{(j)})]$.

Step 4. Obtain $R^{(j)}$ and $h^{(j)}$, where $R^{(j)} \equiv R^{(j)}(t_0)$ and $h^{(j)} \equiv h^{(j)}(t_0)$.

Step 5. Replace j by $j + 1$.

Step 6. Repeat the process from 2 to 5, M times.

Step 7. For $j = 1, \ldots, m$, store the sequence $\left(\alpha^{(j)}, \theta^{(j)}, a^{(j)}, b^{(j)}, R^{(j)}, h^{(j)}\right)$.

Before computing the BEs and BCIs using the generated sequence, it is crucial to eliminate the influence of the initial guesses. To achieve this, we discard the first B generated samples, considering them as a burn-in period. Then, based on the SE loss function, the BEs of the various unknown parameters can be computed as

$$\tilde{\alpha} = \frac{1}{M^*} \sum_{j=B+1}^{M} \alpha^{(j)}, \ \tilde{\theta} = \frac{1}{M^*} \sum_{j=B+1}^{M} \theta^{(j)}, \ \tilde{a} = \frac{1}{M^*} \sum_{j=B+1}^{M} b^{(j)}$$

and

$$\tilde{b} = \frac{1}{M^*} \sum_{j=B+1}^{M} b^{(j)}, \ \tilde{R} = \frac{1}{M^*} \sum_{j=B+1}^{M} R^{(j)}, \ \tilde{h} = \frac{1}{M^*} \sum_{j=B+1}^{M} h^{(j)},$$

where $M^* = M - B$. Moreover, to get the BCIs of the different parameters, we first sort the acquired MCMC samples as $\alpha^{[B+1]} < \ldots, \alpha^{[M]}$, $\theta^{[B+1]} < \ldots, \theta^{[M]}$, $a^{[B+1]} < \ldots, a^{[M]}$, $b^{[B+1]} < \ldots, b^{[M]}$, $R^{[B+1]} < \ldots, R^{[M]}$ and $h^{[B+1]} < \ldots, h^{[M]}$. Then, the $100(1-\tau)\%$ BCIs can be computed as follows:

$$\left[\alpha^{[\tau M^*/2]}, \alpha^{[(1-\tau/2)M^*]}\right], \left[\theta^{[\tau M^*/2]}, \theta^{[(1-\tau/2)M^*]}\right], \left[a^{[\tau M^*/2]}, a^{[(1-\tau/2)M^*]}\right]$$

and

$$\left[b^{[\tau M^*/2]}, b^{[(1-\tau/2)M^*]}\right], \left[R^{[\tau M^*/2]}, R^{[(1-\tau/2)M^*]}\right], \left[h^{[\tau M^*/2]}, h^{[(1-\tau/2)M^*]}\right].$$

5. Simulation studies

This section evaluates and compares the offered theoretical findings for point and interval estimators about α, θ, $R(t)$, and $h(t)$ based on a series of extensive Monte Carlo simulations.

5.1. Simulation scenarios

This part presents various scenarios for simulating random samples from progressively first-failure censoring via beta-binomial random removals and then analyzing how well acquired estimators perform with those simulated samples. For this objective, following Elshahhat et al. [14], we replicate the PFFC-BBR mechanism 1,000 times from WD(0.75,0.25). At the same time, by taking $t_0 = 0.1$, the true values of $R(t)$ and $h(t)$ are taken as 0.95652 and 0.33343, respectively. Further, each offered estimated of α, θ, $R(t)$, or $h(t)$ is assessed based on several options of r(no. of groups), k(group size), and d(effective censoring), such as $r(= 40, 80)$, $k(= 2, 4)$, and d is specified as a failure percentage (FP%) such as $\frac{d}{r} = 25$, 50, and 75%. Furthermore, to examine the effect of the beta-binomial parameters on the estimation results, two different sets of BB(a, b) are utilized; namely *BB*-I:(0.2,0.8) and *BB*-II:(2,1).

After gathering 1,000 PFFC-BBR samples using R software, we install two crucial packages to compute the estimates of α, θ, $R(t)$, and $h(t)$, namely, 'CODA' and 'maxLik' packages by Plummer et al. [28] and Henningsen and Toomet [29], respectively. In Bayes' computations, according to Section 4, we gather 12,000 MCMC variates and reject the first 2,000 MCMC variates for each parameter in accordance with the suggested MCMC technique. Then, the MCMC estimates of α, θ, $R(t)$, and $h(t)$ are computed, along with the corresponding 95% BCIs.

In Bayesian framework, the elicitation process to identify the hyperparameter value is the major issue. Assuming that a large number of complete samples (of size n) are observed, MLEs for α and θ are obtained based on each simulated sample. Next, we equate the mean and variance of $\hat{\alpha}$ and $\hat{\theta}$ to the mean and variance of the gamma prior distribution. As a result, the hyperparameter values of $\nu_j, \omega_j,\ j = 1, 2$, are determined by applying the election technique of prior-parameter value suggested by Nassar and Elshahhat [26]. Now, we generate 10,000 complete samples (say, each of size 50) from WD(0.75,0.25) as past samples for each plausible value of α and θ. As a result, we assigned the values of ν_1, ν_2, ω_1, and ω_2 as 75.9853, 16.1922, 98.5269, and 65.1808, respectively.

Now, we evaluate the point and interval estimates computed for α, θ, $R(t)$, and $h(t)$ (say $\aleph$) based on the following criteria:

- The average estimate (AvE):

$$\text{AvE}(\grave{\aleph}) = \frac{1}{1000}\sum_{i=1}^{1000} \grave{\aleph}^{[i]}.$$

- Root mean squared-error (RMSE):

$$\text{RMSE}(\grave{\aleph}) = \sqrt{\frac{1}{1000}\sum_{i=1}^{1000}\left(\grave{\aleph}^{[i]} - \aleph\right)^2}.$$

- Average relative absolute bias (ARAB):

$$\text{ARAB}(\grave{\aleph}) = \frac{1}{1000}\sum_{i=1}^{1000}\grave{\aleph}^{-1}\left|\grave{\aleph}^{[i]} - \aleph\right|.$$

- Average interval length (AIL):

$$\text{AIL}_{(1-\alpha)\%}(\aleph) = \frac{1}{1000}\sum_{i=1}^{1000}\left(\mathcal{U}_{\grave{\aleph}^{[i]}} - \mathcal{L}_{\grave{\aleph}^{[i]}}\right).$$

- Coverage percentage (CP):

$$\text{CP}_{(1-\tau)\%}(\aleph) = \frac{1}{1000}\sum_{i=1}^{1000}\mathbb{I}_{\left(\mathcal{L}_{\grave{\aleph}^{[i]}};\mathcal{U}_{\grave{\aleph}^{[i]}}\right)}(\aleph).$$

where $\grave{\aleph}^{[i]}$ is the calculated estimate of $\aleph$ at the ith sample, $\mathbb{I}(\cdot)$ is the indicator, and $(\mathcal{L}(\cdot),\mathcal{U}(\cdot))$ refers to (lower,upper) ACI (or BCI) bounds.

5.2. Results and discussions

In the first, second, and third columns of Tables 1–4, the AvEs, RMSEs, and ARABs of α, θ, $R(t)$, and $h(t)$ are tabulated, respectively. In the first and second columns of Tables 5–8, the AILs and CPs of α, θ, $R(t)$, and $h(t)$ are provided, respectively. From Tables 1–8, in terms of lowest RMSE, ARAB, and AIL values as well as highest CP values, we report the following assessments:

- All acquired point (or interval) estimates of α, θ, $R(t)$, or $h(t)$ behaved satisfactorily.
- As r(or FP%) grows, the accuracy of all proposed estimates becomes even better.
- The Bayesian estimates based on gamma conjugate priors outperform the frequentist estimates because prior information is provided.
- As k grows, it is noted that:
  - For point estimates, the RMSEs and ARABs of α decrease while those of θ, $R(t)$, or $h(t)$ increase;
  - For interval estimates, the AILs of α, θ, $R(t)$, and $h(t)$ decreased while their CPs grew.
- Researchers who want to obtain highly efficient and accurate estimates of model parameters or reliability indices are advised to increase the number and/or size of the groups under investigation.
- As BB(a, b) grow, it is noted that:
  - For point estimates, the RMSEs and ARABs of θ increase while those of α, $R(t)$, or $h(t)$ decrease;
  - For interval estimates, the AILs of α decrease while those of θ, $R(t)$, or $h(t)$ increase; whereas the CPs of α increase while those of θ, $R(t)$, or $h(t)$ decrease.

- In most simulation scenarios, the estimated CP value of α, θ, $R(t)$, or $h(t)$ is close to the pre-specified nominal 95% level.
- Finally, employing the Bayes paradigm via MH within Gibbs sampling to offer point (or interval) estimates of the Weibull population parameters is recommended once the proposed PFFC-BBR sample is available.

Table 1. The point results of α.

k	r	FP%	MLE			Bayes'		
					BB-I			
2	40	25%	1.067	1.073	1.174	1.120	0.848	1.078
		50%	0.884	0.791	0.867	0.937	0.691	0.866
		75%	0.722	0.586	0.756	0.903	0.433	0.480
	80	25%	1.073	0.498	0.656	1.256	0.287	0.334
		50%	0.799	0.410	0.463	0.966	0.214	0.266
		75%	0.707	0.246	0.326	0.791	0.166	0.185
4	40	25%	1.067	0.884	0.974	1.119	0.788	0.795
		50%	0.884	0.676	0.790	0.927	0.626	0.679
		75%	0.722	0.534	0.682	0.920	0.413	0.438
	80	25%	1.073	0.435	0.594	1.247	0.257	0.311
		50%	0.799	0.386	0.459	0.949	0.204	0.228
		75%	0.707	0.226	0.317	0.796	0.147	0.163
					BB-II			
2	40	25%	1.303	0.860	1.093	1.137	0.718	0.895
		50%	0.831	0.659	0.825	1.054	0.477	0.539
		75%	0.717	0.547	0.732	0.993	0.367	0.395
	80	25%	0.921	0.437	0.625	1.056	0.263	0.291
		50%	0.724	0.366	0.451	0.877	0.201	0.216
		75%	0.655	0.218	0.318	0.796	0.129	0.116
4	40	25%	1.303	0.829	0.879	1.145	0.730	0.785
		50%	0.831	0.606	0.795	1.039	0.477	0.524
		75%	0.717	0.515	0.610	0.987	0.367	0.329
	80	25%	0.921	0.393	0.562	1.052	0.267	0.247
		50%	0.724	0.322	0.436	0.870	0.201	0.209
		75%	0.655	0.195	0.302	0.781	0.121	0.103

Table 2. The point results of θ.

k	r	FP%	MLE			Bayes'		
					BB-I			
2	40	25%	0.347	0.190	0.717	0.249	0.178	0.687
		50%	0.313	0.166	0.639	0.234	0.151	0.583
		75%	0.321	0.163	0.619	0.484	0.132	0.568
	80	25%	0.412	0.152	0.594	0.421	0.124	0.460
		50%	0.361	0.147	0.563	0.238	0.119	0.419
		75%	0.428	0.137	0.517	0.405	0.097	0.367
4	40	25%	0.277	0.219	0.865	0.325	0.207	0.824
		50%	0.324	0.211	0.838	0.316	0.198	0.791
		75%	0.337	0.204	0.812	0.244	0.185	0.753
	80	25%	0.412	0.200	0.797	0.290	0.180	0.716
		50%	0.361	0.196	0.782	0.414	0.171	0.668
		75%	0.428	0.174	0.739	0.367	0.161	0.615
					BB-II			
2	40	25%	0.276	0.194	0.739	0.282	0.183	0.776
		50%	0.377	0.188	0.691	0.295	0.176	0.601
		75%	0.437	0.170	0.624	0.341	0.157	0.499
	80	25%	0.311	0.159	0.599	0.305	0.147	0.462
		50%	0.406	0.150	0.558	0.268	0.137	0.412
		75%	0.463	0.146	0.523	0.299	0.125	0.337
4	40	25%	0.276	0.222	0.885	0.263	0.218	0.860
		50%	0.377	0.216	0.845	0.361	0.213	0.834
		75%	0.437	0.209	0.832	0.286	0.209	0.814
	80	25%	0.311	0.206	0.820	0.218	0.191	0.760
		50%	0.406	0.202	0.795	0.244	0.184	0.733
		75%	0.463	0.197	0.786	0.232	0.182	0.724

Table 3. The point results of $R(t)$.

k	r	FP%	MLE			Bayes'		
					BB-I			
2	40	25%	0.993	0.042	0.048	0.951	0.039	0.040
		50%	0.989	0.041	0.045	0.909	0.037	0.038
		75%	0.985	0.038	0.042	0.957	0.034	0.035
	80	25%	0.930	0.035	0.039	0.947	0.032	0.035
		50%	0.964	0.034	0.034	0.946	0.030	0.030
		75%	0.985	0.033	0.032	0.914	0.029	0.030
4	40	25%	0.972	0.046	0.051	0.981	0.042	0.043
		50%	0.957	0.044	0.049	0.976	0.040	0.042
		75%	0.940	0.042	0.045	0.947	0.039	0.041
	80	25%	0.965	0.041	0.042	0.938	0.038	0.040
		50%	0.948	0.038	0.040	0.971	0.036	0.037
		75%	0.926	0.037	0.038	0.922	0.033	0.035
					BB-II			
2	40	25%	0.995	0.041	0.045	0.989	0.038	0.039
		50%	0.989	0.038	0.041	0.965	0.036	0.038
		75%	0.984	0.036	0.038	0.919	0.034	0.034
	80	25%	0.992	0.034	0.036	0.925	0.031	0.031
		50%	0.986	0.031	0.033	0.948	0.029	0.029
		75%	0.982	0.030	0.031	0.987	0.026	0.026
4	40	25%	0.975	0.042	0.047	0.945	0.040	0.041
		50%	0.943	0.040	0.045	0.941	0.038	0.039
		75%	0.921	0.039	0.043	0.957	0.037	0.038
	80	25%	0.961	0.038	0.041	0.962	0.036	0.037
		50%	0.930	0.036	0.042	0.971	0.034	0.036
		75%	0.908	0.033	0.040	0.943	0.031	0.033

Table 4. The point results of $h(t)$.

k	r	FP%	MLE			Bayes'		
					BB-I			
2	40	25%	0.339	0.291	0.849	0.290	0.283	0.822
		50%	0.501	0.280	0.824	0.326	0.267	0.774
		75%	0.462	0.271	0.805	0.351	0.255	0.727
	80	25%	0.386	0.268	0.788	0.353	0.243	0.702
		50%	0.479	0.238	0.626	0.311	0.233	0.591
		75%	0.432	0.229	0.621	0.291	0.221	0.609
4	40	25%	0.271	0.311	0.932	0.227	0.308	0.919
		50%	0.401	0.307	0.920	0.265	0.297	0.884
		75%	0.499	0.301	0.900	0.397	0.295	0.876
	80	25%	0.386	0.300	0.895	0.349	0.287	0.856
		50%	0.379	0.285	0.850	0.333	0.282	0.838
		75%	0.316	0.271	0.811	0.382	0.275	0.805
					BB-II			
2	40	25%	0.257	0.280	0.826	0.363	0.277	0.807
		50%	0.351	0.261	0.758	0.401	0.248	0.722
		75%	0.365	0.243	0.698	0.391	0.238	0.706
	80	25%	0.373	0.221	0.644	0.363	0.214	0.696
		50%	0.459	0.213	0.610	0.264	0.204	0.585
		75%	0.373	0.193	0.562	0.406	0.187	0.547
4	40	25%	0.257	0.310	0.923	0.349	0.306	0.916
		50%	0.351	0.298	0.888	0.329	0.289	0.861
		75%	0.365	0.285	0.848	0.351	0.283	0.846
	80	25%	0.373	0.275	0.822	0.463	0.279	0.836
		50%	0.359	0.270	0.804	0.279	0.276	0.812
		75%	0.308	0.266	0.795	0.345	0.261	0.781

Table 5. The interval results of α.

k	r	FP%	95% ACI		95% BCI	
			BB-I			
2	40	25%	1.305	0.896	1.079	0.900
		50%	1.149	0.902	0.879	0.907
		75%	0.849	0.909	0.729	0.912
	80	25%	0.710	0.912	0.470	0.915
		50%	0.491	0.915	0.436	0.916
		75%	0.343	0.918	0.246	0.922
4	40	25%	1.153	0.901	0.872	0.909
		50%	0.783	0.908	0.646	0.916
		75%	0.675	0.915	0.516	0.920
	80	25%	0.491	0.918	0.425	0.924
		50%	0.396	0.921	0.337	0.927
		75%	0.322	0.925	0.215	0.931
			BB-II			
2	40	25%	1.125	0.905	0.791	0.912
		50%	0.743	0.912	0.607	0.917
		75%	0.625	0.915	0.468	0.919
	80	25%	0.527	0.917	0.433	0.920
		50%	0.414	0.920	0.347	0.923
		75%	0.320	0.922	0.212	0.925
4	40	25%	0.974	0.911	0.786	0.921
		50%	0.641	0.918	0.590	0.926
		75%	0.492	0.921	0.456	0.928
	80	25%	0.450	0.923	0.409	0.929
		50%	0.368	0.927	0.286	0.932
		75%	0.283	0.930	0.192	0.934

Table 6. The interval results of θ.

k	r	FP%	95% ACI		95% BCI	
			BB-I			
2	40	25%	0.181	0.942	0.146	0.945
		50%	0.171	0.944	0.134	0.946
		75%	0.144	0.947	0.128	0.948
	80	25%	0.124	0.950	0.116	0.951
		50%	0.105	0.951	0.088	0.953
		75%	0.094	0.953	0.064	0.956
4	40	25%	0.080	0.951	0.058	0.954
		50%	0.066	0.953	0.054	0.955
		75%	0.061	0.956	0.053	0.958
	80	25%	0.051	0.960	0.047	0.962
		50%	0.047	0.961	0.042	0.962
		75%	0.044	0.963	0.034	0.964
			BB-II			
2	40	25%	0.271	0.937	0.180	0.941
		50%	0.236	0.939	0.162	0.943
		75%	0.175	0.943	0.138	0.946
	80	25%	0.135	0.945	0.121	0.947
		50%	0.118	0.946	0.095	0.950
		75%	0.101	0.948	0.080	0.952
4	40	25%	0.157	0.946	0.070	0.950
		50%	0.125	0.948	0.068	0.953
		75%	0.086	0.952	0.064	0.954
	80	25%	0.070	0.954	0.055	0.956
		50%	0.056	0.955	0.049	0.959
		75%	0.051	0.956	0.037	0.962

Table 7. The interval results of $R(t)$.

k	r	FP%	95% ACI		95% BCI	
			BB-I			
2	40	25%	0.033	0.964	0.029	0.966
		50%	0.026	0.966	0.022	0.968
		75%	0.023	0.967	0.020	0.969
	80	25%	0.022	0.968	0.016	0.971
		50%	0.019	0.969	0.013	0.972
		75%	0.016	0.971	0.011	0.973
4	40	25%	0.015	0.974	0.013	0.975
		50%	0.012	0.976	0.011	0.977
		75%	0.010	0.977	0.008	0.979
	80	25%	0.009	0.978	0.007	0.980
		50%	0.008	0.979	0.006	0.981
		75%	0.007	0.981	0.005	0.982
			BB-II			
2	40	25%	0.037	0.962	0.034	0.964
		50%	0.029	0.964	0.025	0.966
		75%	0.027	0.965	0.022	0.967
	80	25%	0.023	0.967	0.017	0.969
		50%	0.020	0.969	0.015	0.970
		75%	0.017	0.970	0.012	0.972
4	40	25%	0.023	0.972	0.017	0.974
		50%	0.019	0.974	0.015	0.976
		75%	0.014	0.976	0.011	0.977
	80	25%	0.013	0.977	0.009	0.978
		50%	0.010	0.978	0.008	0.979
		75%	0.008	0.979	0.007	0.980

Table 8. The interval results of $h(t)$.

k	r	FP%	95% ACI		95% BCI	
			BB-I			
2	40	25%	0.245	0.922	0.204	0.925
		50%	0.214	0.926	0.193	0.927
		75%	0.187	0.928	0.165	0.930
	80	25%	0.168	0.931	0.143	0.933
		50%	0.144	0.933	0.125	0.936
		75%	0.137	0.934	0.109	0.939
4	40	25%	0.115	0.928	0.082	0.932
		50%	0.089	0.932	0.077	0.934
		75%	0.076	0.934	0.072	0.936
	80	25%	0.072	0.938	0.068	0.939
		50%	0.069	0.940	0.055	0.942
		75%	0.066	0.941	0.046	0.944
			BB-II			
2	40	25%	0.331	0.914	0.219	0.924
		50%	0.295	0.919	0.208	0.925
		75%	0.199	0.927	0.170	0.929
	80	25%	0.173	0.930	0.151	0.931
		50%	0.159	0.932	0.128	0.934
		75%	0.144	0.933	0.114	0.937
4	40	25%	0.193	0.922	0.129	0.927
		50%	0.183	0.925	0.104	0.931
		75%	0.147	0.931	0.085	0.934
	80	25%	0.085	0.935	0.077	0.936
		50%	0.074	0.937	0.070	0.938
		75%	0.067	0.939	0.053	0.942

6. Real data applications

The main goals of this part are to demonstrate the estimators' usefulness in real-world scenarios and to demonstrate the estimating methodologies' worth. This part so examines the examination of two real datasets from the clinical and chemical sectors.

6.1. Bladder cancer

A tumor, or the development of abnormal tissue, that forms in the bladder lining is called bladder cancer. The tumor may occasionally spread into the bladder muscle. It is the most frequent urologic cancer, with the greatest incidence of cancer recurrence. This application analyzes a dataset representing the remission times (in months) of a sample of 128 bladder cancer patients; see Table 9.

This set of bladder cancer remission times (BCRTs) is available in Lee and Wang [30].

Table 9. Bladder cancer remission times.

0.08	0.20	0.40	0.50	0.51	0.81	0.90	1.05	1.19	1.26	1.35	1.40
1.46	1.76	2.02	2.02	2.07	2.09	2.23	2.26	2.46	2.54	2.62	2.64
2.69	2.69	2.75	2.83	2.87	3.02	3.25	3.31	3.36	3.36	3.48	3.52
3.57	3.64	3.70	3.82	3.88	4.18	4.23	4.26	4.33	4.34	4.40	4.50
4.51	4.87	4.98	5.06	5.09	5.17	5.32	5.32	5.34	5.41	5.41	5.49
5.62	5.71	5.85	6.25	6.54	6.76	6.93	6.94	6.97	7.09	7.26	7.28
7.32	7.39	7.59	7.62	7.63	7.66	7.87	7.93	8.26	8.37	8.53	8.65
8.66	9.02	9.22	9.47	9.74	10.06	10.34	10.66	10.75	11.25	11.64	11.79
11.98	12.02	12.03	12.07	12.63	13.11	13.29	13.80	14.24	14.76	14.77	14.83
15.96	16.62	17.12	17.14	17.36	18.10	19.13	20.28	21.73	22.69	23.63	25.74
25.82	26.31	32.15	34.26	36.66	43.01	46.12	79.05				

To check if BCRTs data fit the WD(α, θ), the Kolmogorov–Smirnov (K–S) statistic and associated P-value are computed before proceeding. To begin, from Table 9, the MLEs (with their standard-errors (St.Ers)) of α and θ are 1.0475(0.0675) and 0.0939(0.0191), respectively. Consequently, the K–S(P-value) is 0.0699(0.558). As a result, the Weibull lifetime model fits the BCRTs data adequately.

Additionally, from Table 9, the estimated/empirical PDF, the estimated/empirical RF, and contour plots are shown in Figure 2. It supports the fit result and confirms that the Weibull model is suitable to analyze the BCRTs dataset. Figure 2(a) shows that the estimated Weibull density line captured the BCRTs histograms; Figure 2(b) shows that the estimated Weibull reliability line is quite close to its empirical line; Figure 2(c) shows that the MLEs $\hat{\alpha} \cong 1.0475$ and $\hat{\theta} \cong 0.0939$ existed and are unique.

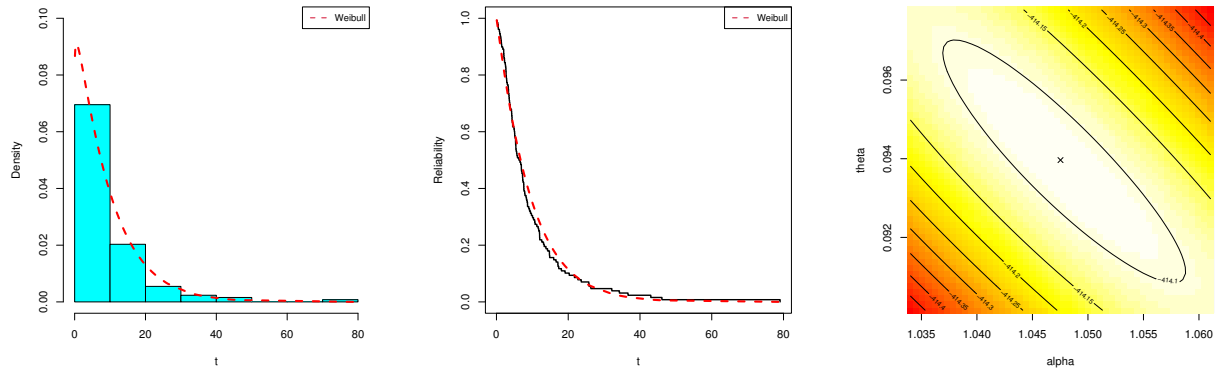

(a) PDF (b) RF (c) Contour

Figure 2. Fitting diagrams of the WD from BCRTs dataset.

Now, to calculate the theoretical results of Weibull parameters of life (α, θ, $R(t)$, $h(t)$) and beta-binomial parameters (a and b), we put the entire BCRTs dataset into a life-test simultaneously, and

randomly classified it into $r = 32$ groups within $k = 4$ items in each group; see Table 10. Next, by assigning $a = b = 2$ and different choices of d, we report three artificial PFFC-BBR samples in Table 11. Specifically, the steps to manually produce a PFFC-BBR sample; one follows Table 1 in Elshahhat et al. [14].

Table 10. Artificial first-failure samples from BCRTs data.

1	2	3	4	5	6	7	8	9	10	11
6.54	1.05*	3.57	25.82	4.51*	0.08*	13.11	7.63	5.41*	79.05	0.5*
34.26	9.22	19.13	2.07*	17.14	6.76	3.52*	3.7*	11.64	1.46*	5.62
9.74	7.28	2.69*	10.66	7.62	16.62	18.10	9.47	12.07	5.85	10.75
2.23*	4.98	43.01	6.97	5.09	11.98	5.71	32.15	7.32	6.25	2.69
12	13	14	15	16	17	18	19	20	21	22
3.36*	5.32	12.63	3.02	13.29	11.79	9.02	4.26*	4.87	20.28	5.41
7.09	2.54*	7.26	1.76*	5.06	7.39	6.93	7.93	7.66	2.02*	3.25
7.59	26.31	2.83*	12.03	2.46*	0.2*	2.75*	5.17	17.36	3.82	46.12
14.77	4.5	8.66	4.34	14.83	21.73	17.12	14.76	2.87*	10.34	2.62*
23	24	25	26	27	28	29	30	31	32	
1.35*	2.64*	2.02	4.18	0.9*	5.49	8.65	13.8	0.81*	2.09	
8.37	3.36	1.4*	3.88	5.32	2.26	23.63	10.06	4.33	1.19*	
4.4	25.74	5.34	36.66	7.87	0.51*	0.4*	12.02	15.96	14.24	
8.53	6.94	3.64	3.48*	1.26	8.26	4.23	3.31*	22.69	11.25	

Table 11. Artificial PFFC-BBR samples from BCRTs data.

d	i	1	2	3	4	5	6	7	8	9	10
10	s_i	5	9	0	4	1	3	0	0	0	0
	t_i	0.08	0.20	0.50	0.81	0.90	1.35	1.46	2.02	2.75	3.31
15	i	1	2	3	4	5	6	7	8	9	10
	s_i	4	7	0	3	1	2	0	0	0	0
	t_i	0.08	0.40	0.51	0.90	1.19	1.35	1.46	1.76	2.07	2.54
	i	11	12	13	14	15					
	s_i	0	0	0	0	0					
	t_i	2.69	2.83	3.36	3.52	3.70					
20	i	1	2	3	4	5	6	7	8	9	10
	s_i	3	5	0	2	0	2	0	0	0	0
	t_i	0.08	0.50	0.81	0.90	1.05	1.19	1.35	1.40	1.46	1.76
	i	11	12	13	14	15	16	17	18	19	20
	s_i	0	0	0	0	0	0	0	0	0	0
	t_i	2.02	2.54	2.62	2.64	2.75	2.83	2.87	3.31	3.36	3.48

Since no prior information is available about α, θ, a, and b, the non-informative prior is considered when $\nu_j, \omega_j = 0.001$, $j = 1, 2, 3.4$. Following the MCMC technique described in Section 4, from 40,000 MCMC samples with 10,000 burn-in, the Bayes MCMC estimates are developed. In Table 12, the point estimations (with their St.Ers) and the interval estimations (with their interval lengths (ILs)) of α, θ, $R(t)$, $h(t)$ (at $t_0 = 1$), a, and b are reported. Table 12 shows that the maximum likelihood and Bayes results of α, θ, $R(t)$, $h(t)$, a, or b are highest close to each other. This note is also observed when comparing the 95% ACI with 95% BCI estimates. In terms of minimum St.Ers and ILs, Table 12 indicates that the Bayes' point (or BCI) estimates of all unknown quantities outperform the likelihood estimates.

To demonstrate the existence and uniqueness of the MLEs of Weibull parameters (α,θ) and beta-binomial parameters (a,b), using the PFFCS-BBR sample at $d = 10$ (as an example) from Table 11, Figure 3 depicts the profile log-likelihoods of α, θ, a, and b. It demonstrates that the provided MLEs of α, θ, a, and b exist and are unique.

Table 12. Estimates of α, θ, $R(t)$, $h(t)$, a, and b from BCRTs data.

d	Par.	MLE		MCMC		95% ACI			95% BCI		
		Est.	St.rr	Est.	St.Er	Lower	Upper	IL	Lower	Upper	IL
10	α	1.5412	0.3421	1.5373	0.0202	0.8707	2.2116	1.3409	1.4989	1.5761	0.0772
	θ	0.0868	0.0311	0.0825	0.0165	0.0258	0.1478	0.1220	0.0526	0.1148	0.0623
	$R(t)$	0.9168	0.0285	0.9209	0.0152	0.8609	0.9728	0.1118	0.8915	0.9488	0.0573
	$h(t)$	0.1338	0.0429	0.1268	0.0256	0.0497	0.2179	0.1682	0.0808	0.1766	0.0958
	a	0.1725	0.3421	0.1665	0.0204	0.0025	0.8429	0.8404	0.1290	0.2049	0.0759
	b	0.2716	0.0311	0.2666	0.0203	0.2106	0.3326	0.1220	0.2279	0.3050	0.0772
15	α	1.8005	0.3417	1.7995	0.0100	1.1307	2.4702	1.3395	1.7802	1.8192	0.0390
	θ	0.0548	0.0215	0.0534	0.0083	0.0126	0.0971	0.0844	0.0380	0.0697	0.0317
	$R(t)$	0.9466	0.0204	0.9481	0.0078	0.9067	0.9866	0.0799	0.9326	0.9627	0.0300
	$h(t)$	0.0987	0.0276	0.0961	0.0149	0.0447	0.1528	0.1081	0.0684	0.1255	0.0570
	a	0.0881	0.3417	0.0820	0.0192	0.0007	0.7578	0.7571	0.0478	0.1191	0.0713
	b	0.2383	0.0215	0.2328	0.0204	0.1961	0.2806	0.0844	0.1940	0.2712	0.0771
20	α	1.8382	0.3484	1.7989	0.0100	1.1554	2.5210	1.3656	1.7801	1.8188	0.0387
	θ	0.0310	0.0126	0.0403	0.0160	0.0063	0.0556	0.0493	0.0284	0.0540	0.0257
	$R(t)$	0.9695	0.0122	0.9605	0.0110	0.9456	0.9934	0.0478	0.9474	0.9720	0.0246
	$h(t)$	0.0569	0.0153	0.0725	0.0196	0.0269	0.0870	0.0601	0.0508	0.0971	0.0463
	a	0.1016	0.3484	0.0841	0.0193	0.0012	0.7844	0.7832	0.0481	0.1219	0.0738
	b	0.1702	0.0126	0.2307	0.0214	0.1456	0.1949	0.0493	0.1909	0.2698	0.0788

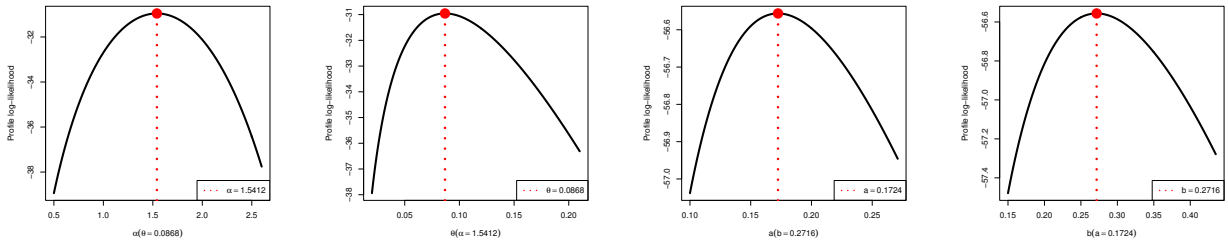

Figure 3. The log-likelihoods of α, θ, a, and b from BCRTs data.

In order to track the convergence of the simulated Markovian chains, using the PFFCS-BBR sample at $d = 10$ (as an example) from Table 11, Figure 4 examines the density and trace plots of α, θ, $R(t)$, $h(t)$, a, and b. The solid and dashed horizontal-lines in each plot indicate the sample average and the two 95% BCI limits, respectively. It demonstrates that the simulated Markov iterations of all unknown quantities are fairly-symmetrical. Once more, we develop several statistics, namely: quartiles Q_i, $i = 1, 2, 3$, mean, mode, standard deviation (St.D), and skewness (Sk.) from the remaining 30,000 iterations of α, θ, $R(t)$, $h(t)$, a, and b; see Table 13. It confirms the results shown in Figure 4 and indicates a convergence within the gathered iterations for each unknown subject.

Table 13. Statistics of α, θ, $R(t)$, $h(t)$, a, and b from BCRTs data.

d	Par.	Mean	Mode	Q_1	Q_2	Q_3	St.Dv.	Sk.
10	α	1.5373	1.4933	1.5236	1.5373	1.5508	0.0198	0.0078
	θ	0.0825	0.0723	0.0713	0.0822	0.0931	0.0160	0.1611
	$R(t)$	0.9209	0.9302	0.9111	0.9211	0.9312	0.0147	-0.1147
	$h(t)$	0.1268	0.1080	0.1096	0.1261	0.1431	0.0246	0.1648
	a	0.1665	0.1337	0.1532	0.1664	0.1797	0.0195	0.0285
	b	0.2666	0.2118	0.2535	0.2665	0.2798	0.0197	-0.0070
15	α	1.7995	1.7754	1.7927	1.7995	1.8062	0.0099	0.0075
	θ	0.0534	0.0466	0.0477	0.0533	0.0589	0.0081	0.1163
	$R(t)$	0.9481	0.9477	0.9428	0.9481	0.9534	0.0077	-0.0927
	$h(t)$	0.0961	0.0827	0.0858	0.0959	0.1059	0.0146	0.1161
	a	0.0820	0.0572	0.0694	0.0815	0.0941	0.0182	0.1405
	b	0.2328	0.1723	0.2196	0.2329	0.2460	0.0197	-0.0326
20	α	1.7989	1.8129	1.7921	1.7988	1.8058	0.0099	0.0730
	θ	0.0403	0.0293	0.0355	0.0400	0.0446	0.0067	0.1985
	$R(t)$	0.9605	0.9712	0.9564	0.9608	0.9651	0.0064	-0.1790
	$h(t)$	0.0725	0.0531	0.0639	0.0720	0.0803	0.0120	0.1935
	a	0.0841	0.0572	0.0714	0.0837	0.0968	0.0189	0.0889
	b	0.2307	0.1723	0.2172	0.2308	0.2442	0.0200	-0.0321

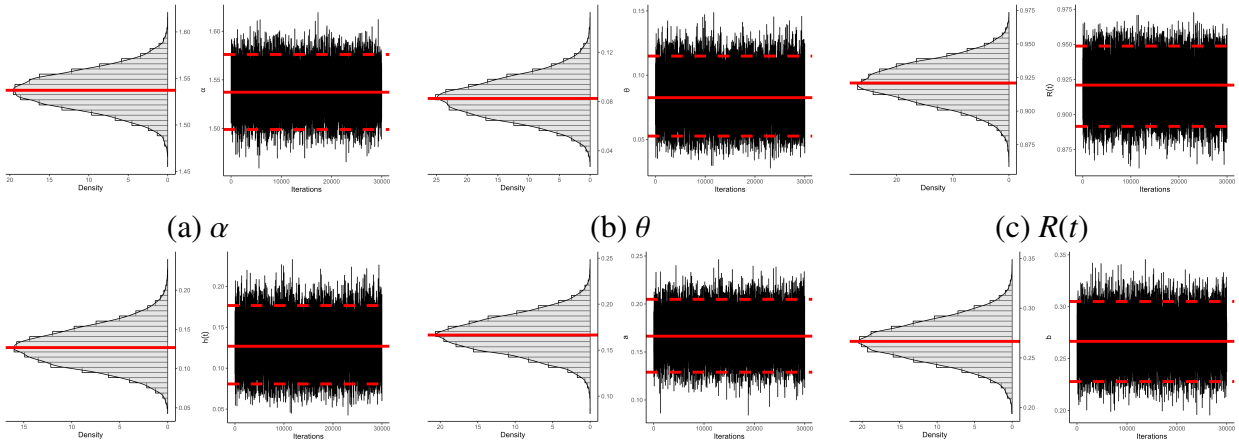

(a) α (b) θ (c) $R(t)$

(d) $h(t)$ (e) a (f) b

Figure 4. The density (left) and trace (right) plots of α, θ, $R(t)$, $h(t)$, a, and b from BCRTs data.

6.2. *Vinyl chloride*

Vinyl chloride is an organochloride that burns easily, is colorless at room temperature, and has an overly pleasant smell. It is also known to be a human carcinogen. In 1835, Henri Victor Regnault and Justus von Liebig made the initial discovery of it. For its commercial applications, including as pipes, packaging materials, and coatings for wire and cable, it cannot be generated naturally and must be created industrially.

In this example, we will examine a data collection of 34 vinyl chloride data points from clean upgradient monitoring wells; see Table 14. Bhaumik et al. [31] provided this dataset and, subsequently, Elshahhat and Elemary [32] and Alotaibi et al. [33] also investigated it.

Table 14. Vinyl chloride (in mg/L) data.

0.1	0.1	0.2	0.2	0.4	0.4	0.4	0.5	0.5	0.5
0.6	0.6	0.8	0.9	0.9	1.0	1.1	1.2	1.2	1.3
1.8	2.0	2.0	2.3	2.4	2.5	2.7	2.9	3.2	4.0
5.1	5.3	6.8	8.0						

From Table 14, the MLEs (with their St.Ers) of α and θ are 1.0102(0.1327) and 0.5262(0.1177), respectively, as well as the K–S(P-value) is 0.0918(0.937). Since the estimated P-value is far from the significance level 5%, we decide that the WD fits the vinyl chloride data satisfactorily. This fact is also supported by four subplots, which are depicted in Figure 5.

Figure 5(a) shows that the density line captured the vinyl chloride data histograms; Figure 5(b) indicates that the estimated reliability line captured its empirical line; Figure 5(c) shows that the MLEs $\hat{\alpha} \cong 1.0102$ and $\hat{\theta} \cong 0.5262$ existed and are unique.

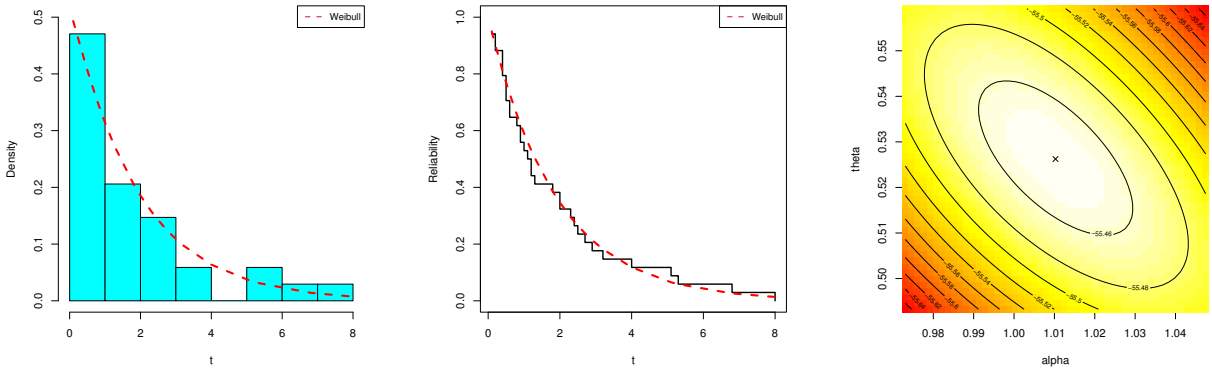

(a) PDF (b) RF (c) Contour

Figure 5. Fitting diagrams of the WD from vinyl chloride dataset.

We now placed the entire vinyl chloride dataset into a life-test simultaneously and randomly grouped it into $r = 17$ with $k = 2$ items in each group; see Table 15. In Table 16, by taking $a = b = 4$, three artificial PFFC-BBR datasets based on various selections of d are provided.

Table 15. Artificial first-failure samples from vinyl chloride data.

1	2	3	4	5	6	7	8	9	10
0.4⋆	0.1⋆	4.0	1.2	2.3	0.5⋆	5.3	0.5⋆	2.0	0.2⋆
2.5	5.1	2⋆	0.1⋆	0.9⋆	1.2	0.6⋆	1.3	0.6⋆	2.9
11	12	13	14	15	16	17			
6.8	1.1⋆	3.2	0.4⋆	1.8	2.4	0.5⋆			
0.8⋆	2.7	0.2⋆	1.0	0.4⋆	0.9⋆	8.0			

Table 16. Artificial PFFC-BBR samples from vinyl chloride data.

d	i	1	2	3	4	5	6	7	8				
8	s_i	3	3	0	1	0	2	0	0				
	t_i	0.1	0.2	0.4	0.4	0.5	0.6	0.9	1.1				
10	i	1	2	3	4	5	6	7	8	9	10		
	s_i	2	2	0	1	0	2	0	0	0	0		
	t_i	0.1	0.2	0.4	0.5	0.5	0.6	0.9	0.9	1.1	2.0		
12	i	1	2	3	4	5	6	7	8	9	10	11	12
	s_i	2	1	0	1	0	1	0	0	0	0	0	0
	t_i	0.1	0.1	0.2	0.4	0.4	0.5	0.5	0.5	0.6	0.8	0.9	0.9

When $\nu_j, \omega_j = 0.001,\ j = 1, 2, 3.4$, the non-informative prior is taken into consideration since there is no prior information available about α, θ, a, and b. Using $(M, B) = (40,000)$, the Bayes MCMC estimates are created using the MCMC approach as outlined in Section 4. In Table 17, the interval and point estimations of α, θ, $R(t)$, $h(t)$ (at $t_0 = 0.1$), a, and b are provided. As Table 17 demonstrates, the Bayes results (along with associated 95% BCI) of α, θ, $R(t)$, $h(t)$, a, or b behave well compared to the MLE (along with associated 95% ACI) results in terms of the lowest St.Er and IL values.

Using the PFFCS-BBR sample at $d = 8$ (as an example) from Table 16, Figure 6 shows that the offered MLEs of the Weibull parameters (α,θ) and beta-binomial parameters (a and b) exist and are unique. Figure 7 indicates that the remaining 30,000 MCMC iterations of α, θ, a, and b are fairly symmetrical, while those of $R(t)$ and $h(t)$ are close to negatively and positively skewed, respectively. Figure 7 supports all findings displayed in Tables 17 and 18.

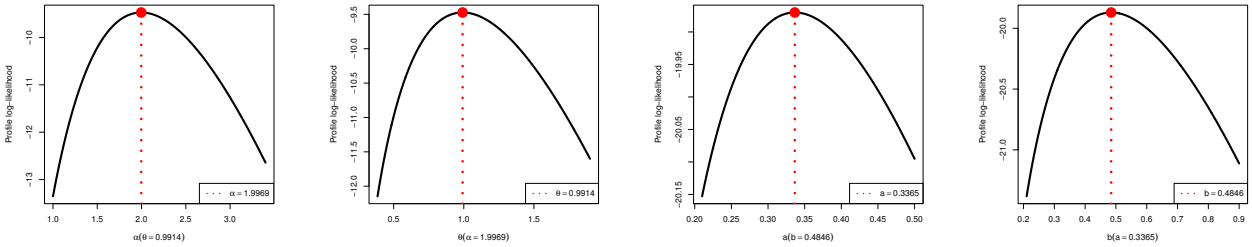

Figure 6. The log-likelihoods of α, θ, a, and b from vinyl chloride data.

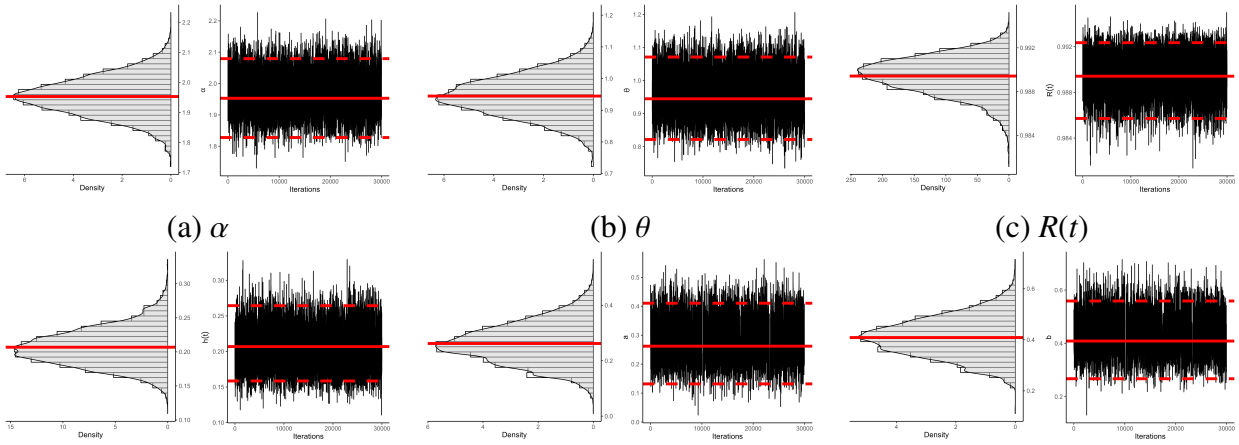

(a) α (b) θ (c) $R(t)$

(d) $h(t)$ (e) a (f) b

Figure 7. The density (left) and trace (right) plots of α, θ, $R(t)$, $h(t)$, a, and b from vinyl chloride data.

Table 17. Estimates of α, θ, $R(t)$, $h(t)$, a, and b from vinyl chloride data.

d	Par.	MLE		MCMC		95% ACI			95% BCI		
		Est.	St.rr	Est.	St.Er	Lower	Upper	IL	Lower	Upper	IL
8	α	1.9969	0.5125	1.9529	0.0774	0.9923	3.0014	2.0091	1.8277	2.0793	0.2516
	θ	0.9914	0.3975	0.9448	0.0791	0.2123	1.7705	1.5582	0.8217	1.0710	0.2493
	$R(t)$	0.9901	0.0104	0.9894	0.0018	0.9697	1.0105	0.0408	0.9857	0.9924	0.0066
	$h(t)$	0.1994	0.1625	0.2068	0.0281	0.0000	0.5179	0.5179	0.1585	0.2643	0.1059
	a	0.3365	0.5125	0.2621	0.1035	0.0000	1.3411	1.3411	0.1319	0.4106	0.2788
	b	0.4846	0.3975	0.4087	0.1070	0.0000	1.2637	1.2637	0.2672	0.5591	0.2918
10	α	1.6250	0.3593	1.9415	0.0835	0.9208	2.3292	1.4084	1.8219	2.0660	0.2442
	θ	0.5725	0.1810	0.9145	0.0998	0.2177	0.9273	0.7096	0.7923	1.0386	0.2464
	$R(t)$	0.9865	0.0119	0.9895	0.0034	0.9633	1.0098	0.0465	0.9858	0.9924	0.0066
	$h(t)$	0.2206	0.1509	0.2043	0.0317	0.0000	0.5163	0.5163	0.1566	0.2623	0.1058
	a	0.2021	0.3593	0.2434	0.1165	0.0000	0.9063	0.9063	0.1052	0.3866	0.2814
	b	0.4229	0.1207	0.4190	0.0982	0.1863	0.6594	0.4731	0.2833	0.5638	0.2805
12	α	2.0238	0.4633	1.9433	0.0833	1.1157	2.9319	1.8163	1.8159	2.0690	0.2531
	θ	1.4467	0.5069	0.6540	0.0625	0.4531	2.4403	1.9872	0.5329	0.7772	0.2443
	$R(t)$	0.9864	0.0124	0.9925	0.0062	0.9622	1.0106	0.0485	0.9897	0.9947	0.0050
	$h(t)$	0.2772	0.1944	0.1456	0.1333	0.0000	0.6583	0.6583	0.1073	0.1915	0.0842
	a	0.3455	0.4633	0.2473	0.1142	0.0000	1.2536	1.2536	0.1102	0.3945	0.2843
	b	0.7452	0.5069	0.4505	0.0793	0.0000	1.7388	1.7388	0.3120	0.5923	0.2803

Table 18. Statistics of α, θ, $R(t)$, $h(t)$, a, and b from vinyl chloride data.

d	Par.	Mean	Mode	Q_1	Q_2	Q_3	St.Dv.	Sk.
8	α	1.9529	1.8170	1.9106	1.9526	1.9953	0.0637	0.0337
	θ	0.9448	0.7923	0.9015	0.9437	0.9879	0.0639	0.0433
	$R(t)$	0.9894	0.9880	0.9883	0.9895	0.9906	0.0017	-0.4491
	$h(t)$	0.2068	0.2194	0.1879	0.2055	0.2240	0.0271	0.3418
	a	0.2621	0.1443	0.2109	0.2593	0.3097	0.0720	0.2046
	b	0.4087	0.2672	0.3561	0.4079	0.4601	0.0755	0.1271
10	α	1.9415	1.9149	1.8992	1.9411	1.9820	0.0625	0.0137
	θ	0.9145	0.7352	0.8716	0.9153	0.9566	0.0636	-0.0202
	$R(t)$	0.9895	0.9911	0.9884	0.9896	0.9907	0.0017	-0.5461
	$h(t)$	0.2043	0.1712	0.1851	0.2032	0.2210	0.0272	0.4120
	a	0.2434	0.0812	0.1955	0.2404	0.2897	0.0700	0.1874
	b	0.4190	0.3559	0.3671	0.4193	0.4684	0.0731	0.0545
12	α	1.9433	1.7949	1.9003	1.9423	1.9867	0.0638	0.0229
	θ	0.6540	0.6326	0.6107	0.6540	0.6963	0.0621	0.0139
	$R(t)$	0.9925	0.9899	0.9917	0.9926	0.9934	0.0013	-0.4631
	$h(t)$	0.1456	0.1821	0.1305	0.1445	0.1593	0.0215	0.3525
	a	0.2473	0.1461	0.1989	0.2443	0.2939	0.0713	0.1782
	b	0.4505	0.3393	0.4010	0.4516	0.4987	0.0716	0.0207

Lastly, the analysis outputs from the bladder cancer and vinyl chloride datasets corroborate the simulation results and show how the proposed inference approaches can be applied in a real-world scenario in the case of the PFFC-BBR sample.

7. Conclusions

In this paper, we present classical and Bayesian estimate methods for the Weibull distribution when samples are gathered using a progressive first-failure censoring strategy. To address the issue of unrealistic fixed removals, it is assumed in this study that the removals at each time point follow a beta-binomial distribution. Two estimation approaches are used to estimate Weibull parameters such as scale, shape, reliability, and failure rate functions, as well as beta-binomial distribution parameters. The first approach is the commonly used maximum likelihood method. The other approach is the Bayesian estimation method, where Bayes estimates are obtained using squared error loss. A simulation study is conducted and two real datasets are investigated to compare different estimates and highlight the significance of the proposed estimates. The numerical findings revealed that as the beta-binomial parameters increase, the RMSE and ARAB decrease for the shape, reliability, and HRFs, while they increase for the scale parameter. Additionally, it was observed that the average interval length decreases for the shape parameter, but decreases for the other quantities as the beta-binomial parameters increase. This demonstrates how the removal pattern affects the accuracy of estimations. When comparing the

different estimates, it is clear that the Bayesian estimation method outperforms the classical likelihood method in terms of both point and interval estimates for all parameters. It is crucial to highlight that the methods we were discussing are only applicable when the data contains a single cause of failure. If there are multiple causes of failure, it is recommended to analyze the data using a competing risks model. In future work, it is suggested to apply the same methods discussed in this paper to accelerated life tests. For example, it would be of interest to investigate the estimation issues of constant-stress accelerated life tests. Another area for future research is studying the application of these methods when the data has multiple causes of failures. In addition, one can explore the same methods that have been discussed in this paper for different lifetime models, such as gamma, inverse Weibull, and exponentiated exponential distributions. One can use other loss functions to compute the Bayes estimates, for example, LINEX and general entropy loss functions. Currently, there is a shortage of real data in the literature on progressively first-failure censored data with BBRs. As a result, a common approach is to generate censored samples from an existing dataset to illustrate the practical application of the proposed methods. We adopted this approach in our study. For future research, it would be interesting to apply the proposed life-testing experiment to collect progressively first-failure censored data with BBRs and employ the same estimation methods discussed in this paper.

Author contributions

Refah Alotaibi: Conceptualization, methodology, investigation, funding acquisition, writing – original draft; Mazen Nassar: Conceptualization, methodology, investigation, writing – review & editing; Zareen A. Khan: Conceptualization, investigation; Ahmed Elshahhat: Methodology, funding acquisition, writing – original draft. All authors read and approved the final manuscript.

Use of AI tools declaration

The authors declare they have not used Artificial Intelligence (AI) tools in the creation of this article.

Funding

The authors extend their appreciation to the Deanship of Scientific Research and Libraries in Princess Nourah bint Abdulrahman University for funding this research work through the Research Group project, Grant No. (RG-1445-0011).

Acknowledgments

The authors would like to express their gratitude to the editor and referees for their valuable comments. The authors extend their appreciation to the Deanship of Scientific Research and Libraries in Princess Nourah bint Abdulrahman University for funding this research work through the Research Group project, Grant No. (RG-1445-0011). We would like to thank Wejdan Alajlan for her careful reading of the paper and constructive suggestions for improving its results.

Data Availability

The authors confirm that the data supporting the findings of this study are available within the article.

Conflict of interest

There is no conflict of interest.

References

1. U. Balasooriya, Failure-censored reliability sampling plans for the exponential distribution, *J. Stat. Comput. Simul.*, **52** (1995), 337–349. https://doi.org/10.1080/00949659508811684
2. J. W. Wu, W. L. Hung, C. H. Tsai, Estimation of the parameters of the Gompertz distribution under the first failure-censored sampling plan, *Statistics*, **37** (2003), 517–525. https://doi.org/10.1080/02331880310001598864
3. J. W. Wu, W. L. Hung, C. Y. Chen, Approximate MLE of the scale parameter of the truncated Rayleigh distribution under the first failure-censored data, *J. Inf. Optim. Sci.*, **25** (2004), 221–235. https://doi.org/10.1080/02522667.2004.10699604
4. S. J. Wu, C. Kuş, On estimation based on progressive first-failure-censored sampling, *Comput. Statist. Data Anal.*, **53** (2009), 3659–3670. https://doi.org/10.1016/j.csda.2009.03.010
5. M. Dube, H. Krishna, R. Garg, Generalized inverted exponential distribution under progressive first-failure censoring, *J. Stat. Comput. Simul.*, **86** (2016), 1095–1114. https://doi.org/10.1080/00949655.2015.1052440
6. S. Saini, A. Chaturvedi, R. Garg, Estimation of stress-strength reliability for generalized Maxwell failure distribution under progressive first failure censoring, *J. Stat. Comput. Simul.*, **91** (2021), 1366–1393. https://doi.org/10.1080/00949655.2020.1856846
7. M. Nassar, R. Alotaibi, A. Elshahhat, Statistical analysis of alpha power exponential parameters using progressive first-failure censoring with applications, *Axioms*, **11** (2022), 553. https://doi.org/10.3390/axioms11100553
8. S. K. Ashour, A. A. El-Sheikh, A. Elshahhat, Inferences and optimal censoring schemes for progressively first-failure censored Nadarajah-Haghighi distribution, *Sankhya A*, **84** (2022), 885–923. https://doi.org/10.1007/s13171-019-00175-2
9. M. S. Eliwa, E. A. Ahmed, Reliability analysis of constant partially accelerated life tests under progressive first failure type-II censored data from Lomax model: EM and MCMC algorithms, *AIMS Mathematics*, **8** (2023), 29–60. https://doi.org/10.3934/math.2023002
10. N. Alsadat, M. Abu-Moussa, A. Sharawy, On the study of the recurrence relations and characterizations based on progressive first-failure censoring, *AIMS Mathematics*, **9** (2024), 481–494. https://doi.org/10.3934/math.2024026
11. H. K. Yuen, S. K. Tse, Parameters estimation for Weibull distributed lifetimes under progressive censoring with random removals, *J. Stat. Comput. Simul.*, **55** (1996), 57–71. https://doi.org/10.1080/00949659608811749

12. S. R. Huang, S. J. Wu, Estimation of Pareto distribution under progressive first-failure censoring with random removals, *J. Chin. Statist. Assoc.*, **49** (2011), 82—97.

13. S. K. Ashour, A. A. El-Sheikh, A. Elshahhat, Inferences for Weibull lifetime model under progressively first-failure censored data with binomial random removals, *Statist. Optim. Inf. Comput.*, **9** (2020), 47–60. https://doi.org/10.19139/soic-2310-5070-611

14. A. Elshahhat, V. K. Sharma, H. S. Mohammed, Statistical analysis of progressively first-failure-censored data via beta-binomial removals, *AIMS Mathematics*, **8** (2023), 22419–22446. https://doi.org/10.3934/math.20231144

15. S. K. Singh, U. Singh, V. K. Sharma, Expected total test time and Bayesian estimation for generalized Lindley distribution under progressively Type-II censored sample where removals follow the beta-binomial probability law, *Appl. Math. Comput.*, **222** (2013), 402–419. https://doi.org/10.1016/j.amc.2013.07.058

16. I. Usta, H. Gezer, Parameter estimation in Weibull distribution on progressively Type-II censored sample with beta-binomial removals, *Econom. Bus.*, **10** (2016), 505–515.

17. A. Kaushik, U. Singh, S. K. Singh, Bayesian inference for the parameters of Weibull distribution under progressive Type-I interval censored data with beta-binomial removals, *Comm. Statist. Simulation Comput.*, **46** (2017), 3140–3158. https://doi.org/10.1080/03610918.2015.1076469

18. P. K. Vishwakarma, A. Kaushik, A. Pandey, U. Singh, S. K. Singh, Bayesian estimation for inverse Weibull distribution under progressive Type-II censored data with beta-binomial removals, *Aust. J. Stat.*, **47** (2018), 77–94. http://dx.doi.org/10.17713/ajs.v47i1.578

19. P. K. Sangal, A. Sinha, Classical estimation in exponential power distribution under Type-I progressive hybrid censoring with beta-binomial removals, *Int. J. Agricult. Stat. Sci.*, **17** (2021), 1973–1988.

20. X. Jia, D. Wang, P. Jiang, B. Guo, Inference on the reliability of Weibull distribution with multiply Type-I censored data, *Reliab. Eng. Syst. Safety*, **150** (2016), 171–181. https://doi.org/10.1016/j.ress.2016.01.025

21. M. Nassar, M. Abo-Kasem, C. Zhang, S. Dey, Analysis of Weibull distribution under adaptive type-II progressive hybrid censoring scheme, *J. Indian. Soc. Probab. Stat.*, **19** (2018), 25–65. https://doi.org/10.1007/s41096-018-0032-5

22. E. Ramos, P. L. Ramos, F. Louzada, Posterior properties of the Weibull distribution for censored dat, *Stat. Probab. Lett.*, **166** (2020), 108873. https://doi.org/10.1016/j.spl.2020.108873

23. T. Zhu, Statistical inference of Weibull distribution based on generalized progressively hybrid censored data, *J. Comput. Appl. Math.*, **371** (2020), 112705. https://doi.org/10.1016/j.cam.2019.112705

24. J. K. Starling, C. Mastrangelo, Y. Choe, Improving Weibull distribution estimation for generalized Type I censored data using modified SMOTE, *Reliab. Eng. Syst. Safety*, **211** (2021), 107505. https://doi.org/10.1016/j.ress.2021.107505

25. J. Ren, W. Gui, Statistical analysis of adaptive type-II progressively censored competing risks for Weibull models, *Appl. Math. Model.*, **98** (2021), 323–342. https://doi.org/10.1016/j.apm.2021.05.008

26. M. Nassar, A. Elshahhat, Estimation procedures and optimal censoring schemes for an improved adaptive progressively type-II censored Weibull distribution, *J. Appl. Stat.*, **51** (2024), 1664–1688. https://doi.org/10.1080/02664763.2023.2230536

27. A. Xu, B. Wang, D. Zhu, J. Pang, X. Lian, Bayesian reliability assessment of permanent magnet brake under small sample size, *IEEE Trans. Reliab.*, 2024, 1–11. https://doi.org/10.1109/TR.2024.3381072

28. M. Plummer, N. Best, K. Cowles, K. Vines, CODA: Convergence diagnosis and output analysis for MCMC, *R News*, **6** (2006), 7–11.

29. A. Henningsen, O. Toomet, maxLik: A package for maximum likelihood estimation in R, *Comput. Stat.*, **26** (2011), 443–458. https://doi.org/10.1007/s00180-010-0217-1

30. E. T. Lee, J. W. Wang, *Statistical methods for survival data analysis*, John Wiley & Sons, Inc., 2003.

31. D. K. Bhaumik, K. Kapur, R. D. Gibbons, Testing parameters of a gamma distribution for small samples, *Technometrics*, **51** (2009), 326–334. https://doi.org/10.1198/tech.2009.07038

32. A. Elshahhat, B. R. Elemary, Analysis for Xgamma parameters of life under Type-II adaptive progressively hybrid censoring with applications in engineering and chemistry, *Symmetry*, **13** (2021), 2112. https://doi.org/10.3390/sym13112112

33. R. Alotaibi, A. Elshahhat, H. Rezk, M. Nassar, Inferences for alpha power exponential distribution using adaptive progressively type-II hybrid censored data with applications, *Symmetry*, **14** (2022), 651. https://doi.org/10.3390/sym14040651

AIMS Press